

## Mechanism and Kinetics of Stabilization Reactions of Polyacrylonitrile and Related Copolymers IV. Effects of Atmosphere on Isothermal DSC Thermograms and FT-IR Spectral Changes during Stabilization Reaction of Acrylonitrile/Methacrylic Acid Copolymer

Hideto KAKIDA and Kohji TASHIRO\*

Central Technology Research Laboratories, Mitsubishi Rayon Co., Ltd.,  
Otake, Hiroshima 739-0693, Japan

\*Department of Macromolecular Science, Graduate School of Science,  
Osaka University, Toyonaka, Osaka 560-0043, Japan

(Received September 26, 1997)

**ABSTRACT:** Structure formation during the stabilization reactions of the acrylonitrile/methacrylic acid (AN/MAA) copolymer under air, O<sub>2</sub> and N<sub>2</sub> was studied by an organized combination of isothermal DSC thermograms and FT-IR spectra. Under the oxidative atmosphere evolved heat was very large and the conjugated cyclic structure was formed as a stable structure. Particularly in pure O<sub>2</sub> gas the stabilization reaction attained to the most advanced state. Under N<sub>2</sub> the evolved heat was smallest and the resulted structure was thought to be a non-conjugated cyclic imine-enamine tautomerism structure.

**KEY WORDS** Polyacrylonitrile / Acrylonitrile-Methacrylic Acid Copolymer / Carbon Fiber / Stabilization / Differential Scanning Calorimetry / Fourier Transform Infrared Spectroscopy /

Acrylic fibers made of polyacrylonitrile (PAN) containing acidic comonomers such as methacrylic acid (MAA), itaconic acid or acrylic acid are the most commonly used precursors for carbon fibers because of excellent performances of PAN based carbon fibers.<sup>1</sup>

In the production processes of PAN based carbon fibers, stabilization process is most important, because the physical properties of carbon fibers are affected significantly by the conditions of stabilization process. A lot of studies have been reported concerning the stabilization of PAN since 1950.<sup>2,3</sup> According to these papers, acrylic fibers are converted to infusible and non-flammable fibers by heating at 200—300°C for about 1 h in an oxidative atmosphere during stabilization process. Only such stabilized fibers can be heated to carbonization temperature (1000—2000°C).<sup>4</sup>

In these several years, through an organized combination of isothermal DSC exothermic thermograms and FT-IR spectra we have studied the mechanism of stabilization reaction of PAN homopolymer, acrylonitrile (AN)/MAA and AN/acrylamide (AAM) copolymers obtained by aqueous suspension polymerization with a redox initiator,<sup>3,5,6</sup> and the following were indicated: (1) In isothermal DSC exothermic thermograms, induction periods are observed at early time region. During induction, initiation reaction of cyclization occurs. (2) MAA comonomer accelerates the stabilization to high degree where dehydrogenation is preferably accelerated. (3) AAM comonomer accelerates the stabilization only a little more than that of the PAN homopolymer.

In this way, we studied the roles of comonomers in stabilization and the rate of stabilization. It is said also that the precursor fibers are stabilized under an oxidative atmosphere, otherwise the resultant carbon fibers show only inferior performances.

To get information about the effects of atmosphere on stabilization, isothermal DSC thermograms and IR spectral changes were measured under air, N<sub>2</sub>, and O<sub>2</sub>

gas flows.

## EXPERIMENTAL

### Materials

The AN copolymer which contains about 1 mol% MAA was obtained by aqueous suspension polymerization with redox initiator. The weight averaged molecular weight was about  $2 \times 10^5$ . Triad tacticity was  $mm=0.27$ ,  $mr=0.50$ , and  $rr=0.23$  when evaluated by <sup>13</sup>C NMR. The polymer powders filtered through a 400 mesh screen were used for DSC and FT-IR measurements.

### DSC Measurements

Isothermal DSC measurements were carried as described previously.<sup>3,5,6</sup> SEIKO DSC 220C, a kind of heat-flux DSC, was used. To obtain an isothermal thermogram, sample pans were put quickly into the furnace maintained at predetermined temperatures. When the measurements were done under N<sub>2</sub> or O<sub>2</sub> gas flow, the DSC cell was covered with a specially designed box made of poly(methyl methacrylate) sheet (Acrylite) to prevent air leakage. The sample pan was placed for about 1 h in the box under N<sub>2</sub> or O<sub>2</sub> so as to purge air, and then put into the DSC furnace and measurement of isothermal DSC thermogram was started.

### FT-IR Measurements

FT-IR measurements were carried out as described previously.<sup>3,5,6</sup> IR spectra of the samples treated thermally in DSC cell for predetermined periods were measured to get information about structural changes during stabilization. The samples heat-treated in DSC cell under N<sub>2</sub> or O<sub>2</sub> gas were taken out from the DSC cell into the above mentioned specially designed box and held at room temperature under N<sub>2</sub> gas to prevent the additional reaction under air flow.

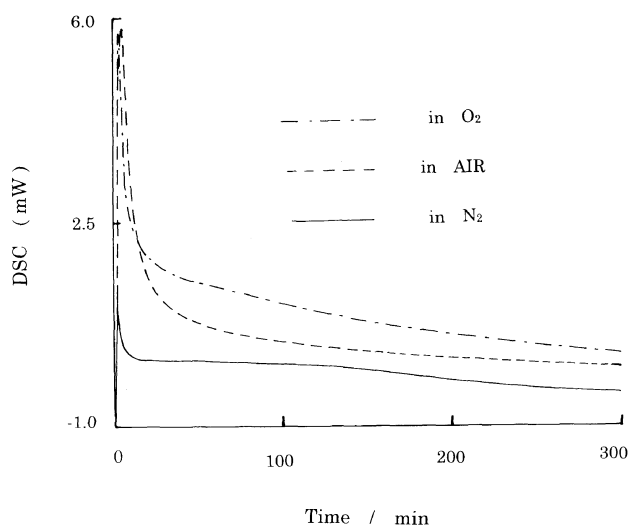


Figure 1. Isothermal DSC thermograms of the AN/MAA copolymer measured under air, O<sub>2</sub> and N<sub>2</sub> at 230°C. Sample weight, 4 mg.

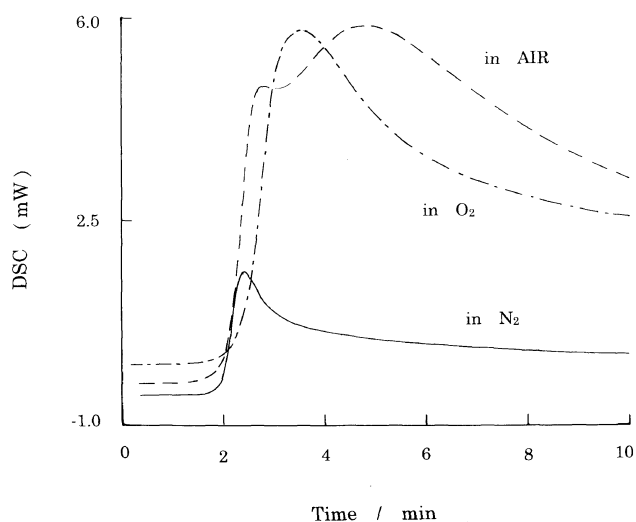


Figure 2. Early time region of isothermal DSC thermograms of the AN/MAA copolymer measured under air, O<sub>2</sub>, and N<sub>2</sub> at 230°C.

## RESULTS AND DISCUSSION

### Effects of Atmosphere on Isothermal DSC Thermograms

Figure 1 shows the isothermal DSC thermograms of the AN/MAA copolymer measured at 230°C under air, O<sub>2</sub> and N<sub>2</sub> gas respectively. In Figure 2 are shown the same thermograms enlarged in the early time region. The isothermal DSC thermogram measured under N<sub>2</sub> shows the smallest exothermic peak at the earliest time among the three. The thermogram under N<sub>2</sub> shows a plateau extending from 10 to 130 min. After the plateau the heat flow continues to decrease very slowly. The thermogram under air flow shows a larger and broader exothermic peak at a later time than that under N<sub>2</sub> flow. In this case the exothermic peak is a little broader than the other two. The thermogram under O<sub>2</sub> shows the peak as large as that under air flow at an earlier time than that under air flow. After the exothermic peak, the heat flow is larger than the other two as seen in Figure 1.

In Figure 2, all thermograms show induction periods, which correspond to the initial flat parts at *ca.* 2 min.

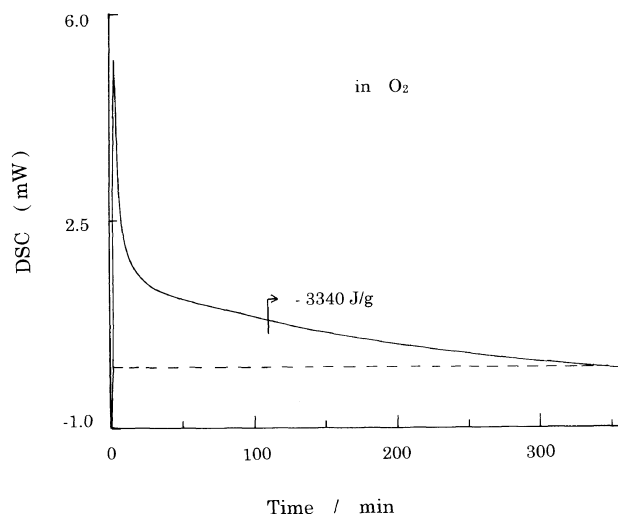


Figure 3. The evolved energy during stabilization under O<sub>2</sub> at 230°C.

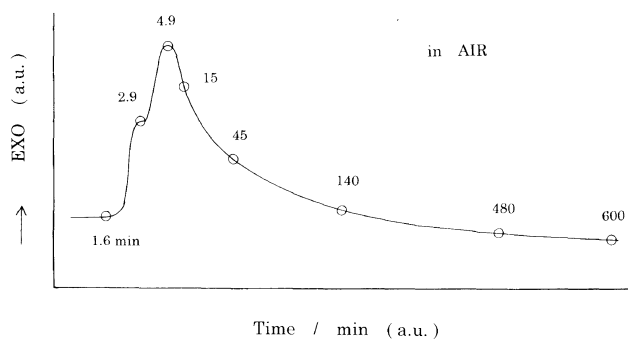
The exothermic peaks of the thermograms obtained under O<sub>2</sub> and N<sub>2</sub> flow are apparently single. The exothermic peak under air flow is composed of a shoulder and main peak, this seems to suggest that in air the both reactions in N<sub>2</sub> and in O<sub>2</sub> occur simultaneously.

Figure 3 shows the isothermal DSC thermogram with total energy evolved during stabilization under O<sub>2</sub> gas. The base line was set as the DSC output level equal to that of the induction period. The evolved total energy is the smallest when the thermogram is obtained under N<sub>2</sub> gas, 1530 J g<sup>-1</sup>. The one under O<sub>2</sub> gas is largest, 3340 J g<sup>-1</sup>, and under air 2520 J g<sup>-1</sup>. This means that stabilization under O<sub>2</sub> gas is highest, while that under N<sub>2</sub> gas lowest.

For stabilization under various gases the following statements may be presented. Under N<sub>2</sub> gas, the main reaction which evolves small amount of heat starts early and completes rapidly, but after that, a small exothermic reaction continues for about 200 min. The formation of stabilized structure is smallest in N<sub>2</sub>. Under O<sub>2</sub> gas, several stabilization reactions seem to occur simultaneously a little later than that under N<sub>2</sub> gas. After the peak, the decrease of heat evolution is slower than the other two cases. So, in this case, the formation of the stabilized structure proceeds slowly but attains much greater degree than the other two cases. Under air, the exothermic peak consists of a shoulder and a main peak, so the reactions under N<sub>2</sub> and O<sub>2</sub> gas apparently occur simultaneously, but the decrease of the heat evolution after peak is faster than under O<sub>2</sub> gas flow. But, the second peak under air is observed later than the exothermic peak under O<sub>2</sub>. Perhaps, this is because that O<sub>2</sub> in air is very little.

### IR Spectral Changes during Stabilization

To clarify the difference of the structural change during stabilization under three atmospheres, the FT-IR spectra were measured along the exothermic DSC thermograms. Figure 4 shows the sampling points on the DSC thermogram, as an example, under air, *i.e.*, the samples were stabilized in DSC cell for the several predetermined periods from 1.6 to 600 min, and followed by FT-IR measurements. The assignments of the



**Figure 4.** Sampling point for FT-IR measurement. Samples are stabilized in DSC cell to the pre-determined time point for FT-IR measurement.

**Table I.** Principal IR bands in solid and degraded PAN, AN/MAA, and AN/AAM copolymer structures

Functional groups	Wavenumber/cm <sup>-1</sup>
NH <sub>2</sub>	3390, 3356
NH	3230
CH <sub>2</sub>	2945, 2920
CH	2895
C≡N (saturated)	2240
C=O (unreacted MAA)	1740
C=O (reacted MAA)	1700
C=O (amide)	1680
N-H (amide)	1620
C=N, C=C mixed	1620 <sup>a</sup>
C=N, C=C, N-H mixed	1580 <sup>a</sup>
CH <sub>2</sub>	1450
CH, NH	1380
C-C, C-N mixed	1250
C=C-H	810

<sup>a</sup> These bands are often not resolved and appear at  $1600 \pm 10 \text{ cm}^{-1}$ .

main IR bands of the degraded PAN and AN/MAA copolymers are summarized in Table I with reference to Fochler *et al.*<sup>7</sup> and Sivy *et al.*<sup>8</sup>

Figure 5 shows changes of the IR spectra measured for the sample stabilized under air. At first, the  $1740 \text{ cm}^{-1}$   $\nu(\text{C}=\text{O})$  band intensity of the unreacted MAA decreases and simultaneously the  $1700 \text{ cm}^{-1}$   $\nu(\text{C}=\text{O})$  band of the reacted MAA appears and increases in intensity. Then,  $1580$  and  $1620 \text{ cm}^{-1}$   $\nu(\text{C}=\text{C})$  and  $\nu(\text{C}=\text{N})$  bands begin to be observed and several minutes later the  $1580$  and  $1620 \text{ cm}^{-1}$  bands converge into the  $1600 \text{ cm}^{-1}$  band. At the same time the  $810 \text{ cm}^{-1}$   $\gamma(\text{C}-\text{H})$  band of  $\text{>C}=\text{C}-\text{H}$  group appears. Then the  $1660 \text{ cm}^{-1}$  band assigned to acridone ring<sup>9</sup> appears. Then the  $1740$  and  $1700 \text{ cm}^{-1}$  bands disappear at about 45 min of stabilization, and at almost the same time the  $2210 \text{ cm}^{-1}$  band, assigned to the  $\alpha$ ,  $\beta$ -unsaturated nitrile groups,<sup>10</sup> begins to be observed. As time of stabilization in DSC cell becomes longer, the  $1600$  and  $810 \text{ cm}^{-1}$  bands increase in intensity, while the  $2240 \text{ cm}^{-1}$  nitrile and  $1450 \text{ cm}^{-1}$  methylene  $\delta(\text{CH}_2)$  bands decrease.

Figure 6 shows changes of the IR spectra measured for the samples stabilized under O<sub>2</sub> gas. The spectral changes resemble that observed under air flow, but the decrease of the intensity of the  $1450 \text{ cm}^{-1}$  methylene band is a little faster than in the air, and the  $2240 \text{ cm}^{-1}$  nitrile band decreases as fast as in air. Appearance of the  $1600$ ,  $810$ , and  $1660 \text{ cm}^{-1}$  bands seems to be a little

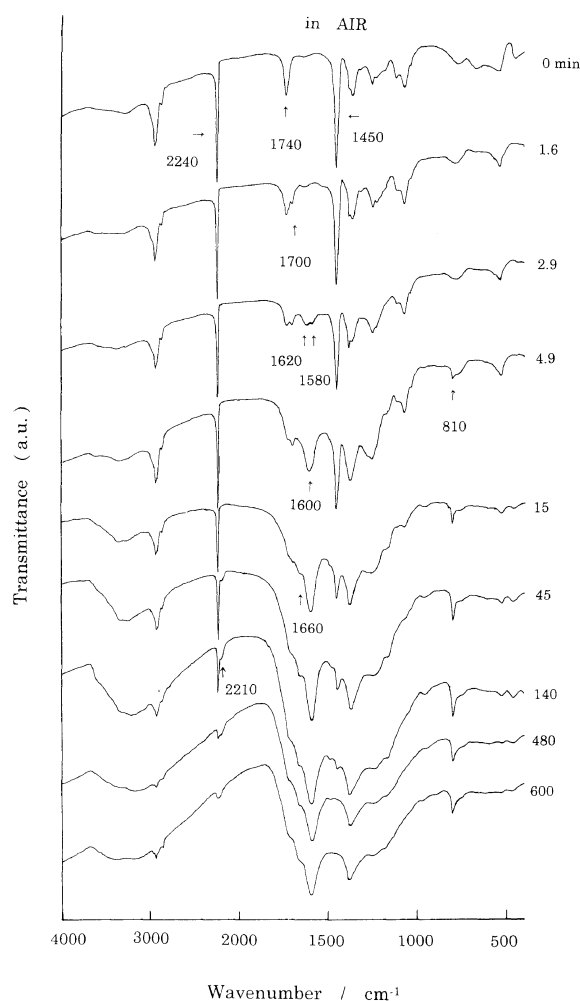


**Figure 5.** IR spectral change during stabilization under air 230°C.

earlier than under air. Also at around 45 min of stabilization, the  $2210 \text{ cm}^{-1}$  band begins to be observed.

Figure 7 shows changes of the IR spectra when the samples were stabilized under N<sub>2</sub> gas flow. The spectral changes are different from those under air or O<sub>2</sub>. The  $1700 \text{ cm}^{-1}$   $\nu(\text{C}=\text{O})$  band of the reacted MAA increases in intensity a little faster than the other two. The  $1740$  and  $1700 \text{ cm}^{-1}$  bands disappear around 45 min of stabilization. Then the band of  $\beta$ -iminonitrile<sup>10</sup> at  $2198 \text{ cm}^{-1}$  begins to appear. Though the nitrile band decreases in intensity as fast as under air or O<sub>2</sub>, the methylene bands at  $1450$  and  $2910 \text{ cm}^{-1}$  decrease much more slowly. The  $1575$  and  $1620 \text{ cm}^{-1}$  bands continue to grow without converging into  $1600 \text{ cm}^{-1}$  band. The rather strong bands which are not observed under air or O<sub>2</sub> are observed at  $3360$ ,  $3200$ ,  $2920$ ,  $2850$ ,  $1255$ ,  $1145$ ,  $790$ , and  $745 \text{ cm}^{-1}$  even after 1000 min of the stabilization treatment. All these bands except  $790 \text{ cm}^{-1}$  band are assigned to the vibrational modes of the degraded PAN under reduced pressure as shown in Table II.<sup>10</sup> The  $790 \text{ cm}^{-1}$  band may be assigned to the vibration of the group analogous to that of the  $810 \text{ cm}^{-1}$  band.

These data of IR spectra show differences in stabilization. Under N<sub>2</sub> gas the nitrile oligomerization proceeds as likely as under air or O<sub>2</sub> gas, but the dehydrogenation occurs only a little. Therefore, the stabilized structure does not become fully conjugated. As shown in

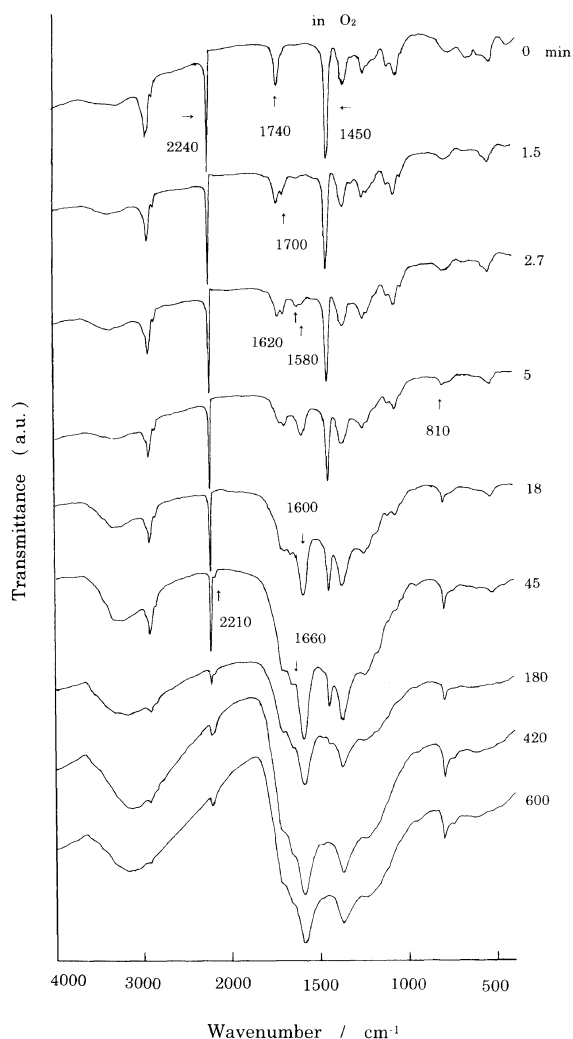


Figure 6. IR spectral change during stabilization under  $O_2$  at  $230^\circ C$ .

Figure 14(c), imine–enamine tautomerism occurs, and  $1620(C=N)$  and  $1575(C=C)$   $cm^{-1}$  bands thus do not converge into single  $1600\text{ cm}^{-1}$  band under  $N_2$  gas 1000 min later. Under air or  $O_2$ , the stabilized molecules become fully conjugated, so the  $1620$  and  $1580\text{ cm}^{-1}$  bands converge into the  $1600\text{ cm}^{-1}$  band.

#### Comparison of Structural Changes

Figures 8, 9, and 10 show intensity changes of the main IR bands during the stabilization in DSC cell under air,  $O_2$  and  $N_2$  respectively. The  $1450\text{ cm}^{-1}$   $\delta(CH_2)$  band intensity decreases rapidly in  $O_2$  flow but maintains intensity even at 1000 min stabilization in  $N_2$  gas. The  $2240\text{ cm}^{-1}$   $\nu(C\equiv N)$  band intensity decreases at the same rate during stabilization in the three gases. This means that the cyclization reaction, *i.e.*, the nitrile oligomerization, proceeds at the same rate in spite of differences of stabilization atmospheres. The bands around  $1600\text{ cm}^{-1}$  behave very differently for the three atmospheres. In the air and  $O_2$ , the  $1580$  and  $1620\text{ cm}^{-1}$  bands are observed separately in the early period and then these bands fuse into the  $1600\text{ cm}^{-1}$  single band immediately. In  $N_2$ , the  $1575$  and  $1620\text{ cm}^{-1}$  bands can be observed even after 1000 min stabilization. Oxygen is considered to affect strongly the formation of the conjugated structure. The  $1660\text{ cm}^{-1}$   $\nu(C=O)$  band assigned to acridone ring

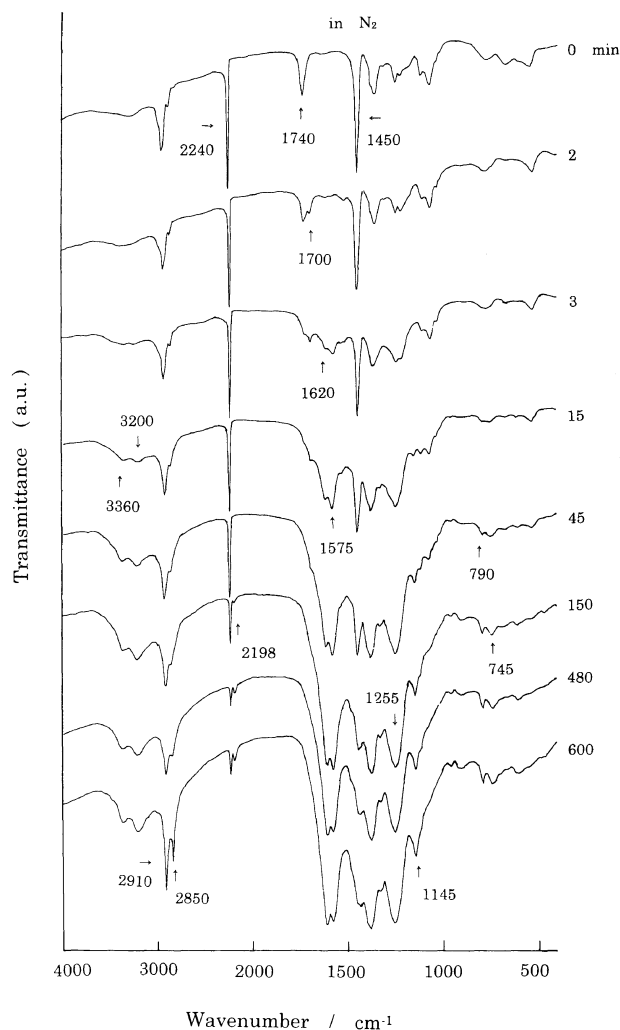


Figure 7. IR spectral change during stabilization under  $N_2$  at  $230^\circ C$ .

Table II. Infrared bands attributable to PAN thermally degraded under reduced pressure

IR bands/ $cm^{-1}$	Tentative assignment
3390	$\nu(NH_2)$
3356	$\nu(NH_2)$
3230	$\nu(NH)$
2930	$\nu(CH_2)$
2870	$\nu(CH_2)$
2240	$\nu(C\equiv N)$
2198	$\beta$ -iminonitrile
1610	mixed mode, predominantly $\nu(C=O) + \nu(C=C)$
1575	mixed mode, predominantly $\nu(C=C) + \delta(NH)$
1485	$\delta(CH_2)$
1450	$\delta(CH_2)$
1385	CH or NH in-plane bending
1325	CH in-plane bend
1250	$\nu(CH_2)$
1150	mixed mode, $\gamma(CN) + \gamma(NH)$
792	
750	$\gamma(CH_2)$

appears early when the sample is stabilized under air or  $O_2$ , but under  $N_2$  the  $1660\text{ cm}^{-1}$  band can not be observed even after the 1000 min stabilization.

Figures 11, 12, and 13 emphasize the early times of Figures 8, 9, and 10. In the case of stabilization under  $O_2$ , the  $1620$  and  $1580\text{ cm}^{-1}$  bands converge into  $1600$

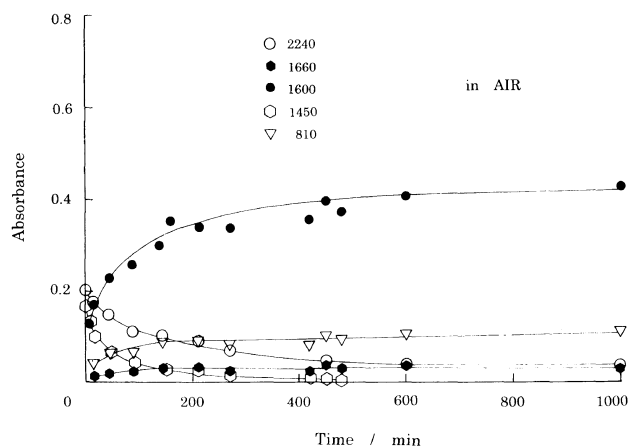


Figure 8. Intensity changes of main IR bands during stabilization under air at 230°C.

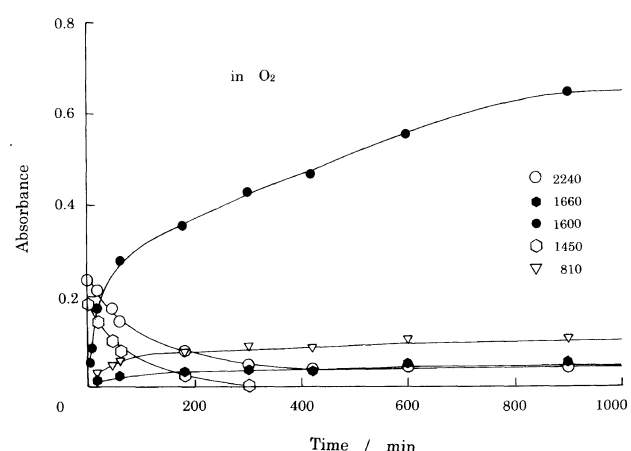


Figure 9. Intensity changes of main IR bands during stabilization under O<sub>2</sub> at 230°C.

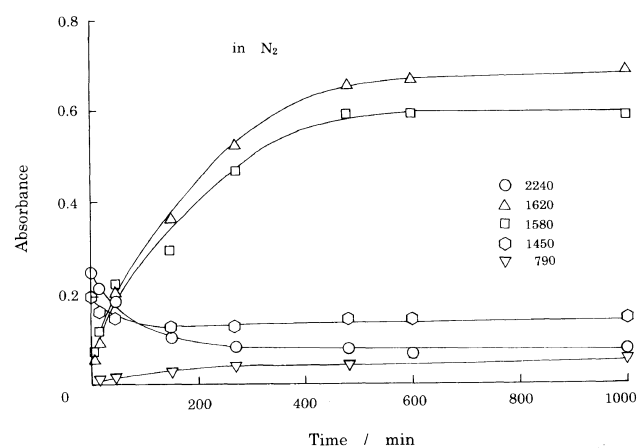


Figure 10. Intensity changes of main IR bands during stabilization under N<sub>2</sub> at 230°C.

cm<sup>-1</sup> band at about 3 min stabilization, earlier than the case under air, and the 810 cm<sup>-1</sup> band appears within 3 min. But, the 1700 cm<sup>-1</sup> ν(C=O) band of the reacted MAA becomes stronger a little later than that in the N<sub>2</sub> atmosphere. The 1740 and 1700 cm<sup>-1</sup> bands can be observed after the 45 min stabilization in all atmospheres.

From the above-mentioned data and by referring to the mechanism presented by Sivy and Coleman,<sup>11</sup>

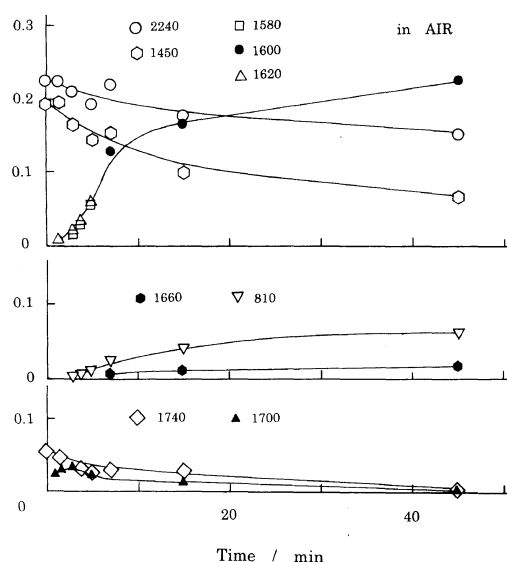


Figure 11. Early time region of intensity changes of main IR bands during stabilization under air at 230°C.

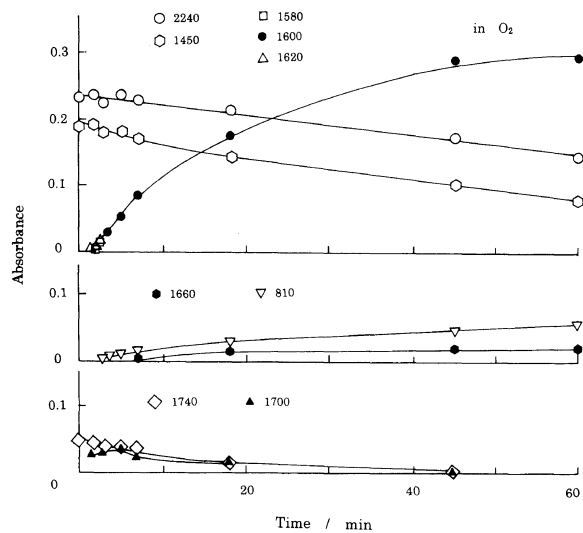


Figure 12. Early time region of intensity changes of main IR bands during stabilization under O<sub>2</sub> at 230°C.

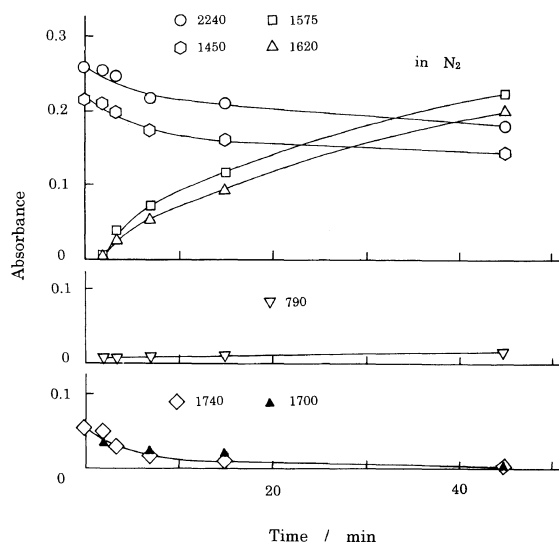


Figure 13. Early time region of intensity changes of main IR bands during stabilization under N<sub>2</sub> at 230°C.

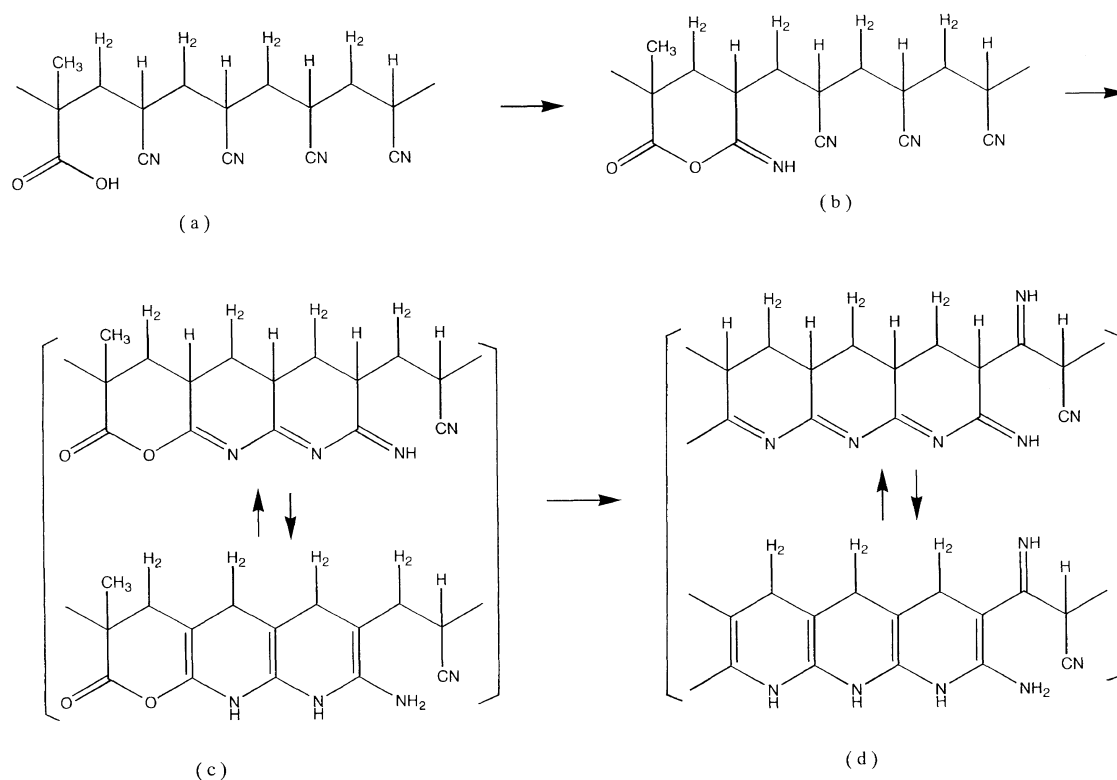


Figure 14. Structural changes during stabilization under  $N_2$  flow at  $230^\circ C$ .

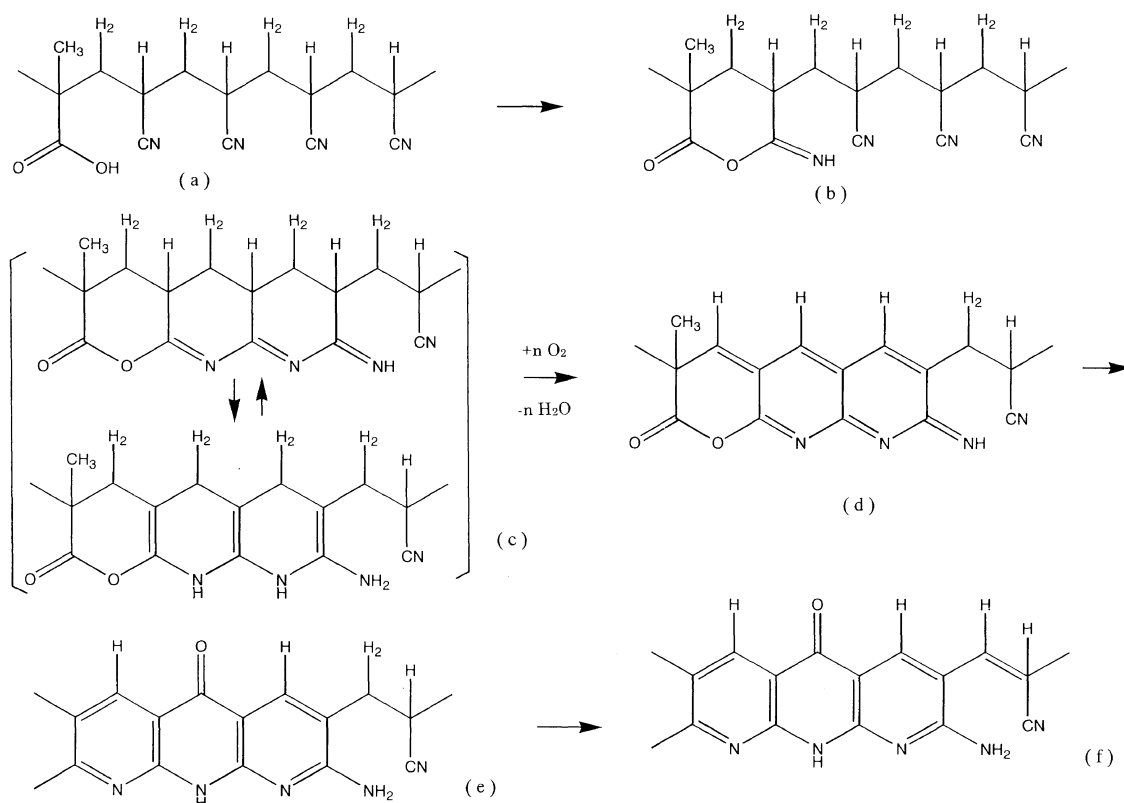


Figure 15. Structural changes during stabilization under  $O_2$  and air at  $230^\circ C$ .

structure formation during stabilization under the three atmospheres may be described as follows.

In  $O_2$ , the exothermic peak of the isothermal DSC thermogram appears a little later and also the  $1700\text{ cm}^{-1}$  reacted MAA band becomes stronger a little later than in  $N_2$  gas, so the reaction of MAA with adjacent nitrile

group occurs later than in  $N_2$ . The reason why stabilization occurs a little later in  $O_2$  than in  $N_2$  is not clear. The cyclization proceeds and a cyclic structure exists as a tautomeric structure as shown in the Figure 15(c), and immediately, as the result of dehydrogenation caused by oxygen, a conjugated structure is formed and

oxygen is introduced into the molecule and remaining nitrile becomes  $\alpha,\beta$ -unsaturated nitrile. This reaction is shown in Figure 15.

In air, structure formation during stabilization is almost the same as under  $O_2$  gas. But the tautomeric structure, Figure 15(c), exists a little longer than in  $O_2$  and also the conjugated structure (d) is formed a little later than in  $O_2$ . Perhaps this is the reason why the exothermic peak of the isothermal DSC thermogram under air flow has a shoulder at a shorter time.

In the case under  $N_2$  gas flow, the  $1700\text{ cm}^{-1}$  band becomes stronger a little earlier than the other two cases, so the initiation reaction of MAA is a little faster than in the other cases, but the reason is not clear. The  $1620$  and  $1575\text{ cm}^{-1}$  bands continue to be observed, and also the  $1450\text{ cm}^{-1}$   $\delta(\text{CH}_2)$  band remains for 1000 min stabilization. Dehydrogenation occurs only a little, so the formation of the conjugated structure cannot occur, and the tautomeric structure, Figure 14(c), continues for 1000 min stabilization. At last the remaining nitrile group becomes  $\beta$ -iminonitrile as shown in Figure 14(d). Structural changes in  $N_2$  atmosphere are shown in Figure 14. Because the triad tacticity of the used polymer is low,  $mm=0.27$ , the average length of isotactic sequence is thought to be short, and when dehydrogenation does not

occur as in Figure 14(c) or (d), successive rings may be only two or three.

The  $3360, 3200, 2920, 2850, 1255, 1145,$  and  $750\text{ cm}^{-1}$  bands, assigned to  $\nu(\text{NH}_2)$ ,  $\nu(\text{NH})$ ,  $\nu(\text{CH}_2)$ ,  $\nu(\text{CH})$ ,  $\delta(\text{CH}_2)$ ,  $\gamma(\text{CN})+\gamma(\text{NH})$ , and  $\gamma(\text{CH}_2)$ , respectively by referring to Table II, can be explained by structure (d) in Figure 14.

## REFERENCES

1. A. Gupta, D. K. Paliwal, and P. Bajaj, *J. Macromol. Sci.*, **C31**, 1 (1991).
2. Z. Bashir, *Carbon*, **29**, 1081 (1991).
3. H. Kakida, K. Tashiro, and M. Kobayashi, *Polym. J.*, **28**, 30 (1996).
4. J. B. Donnet and R. C. Bansal, "Carbon Fiber," 2nd. ed, Marcel Dekker, New York, N.Y., 1990.
5. H. Kakida and K. Tashiro, *Polym. J.*, **29**, 353 (1997).
6. H. Kakida and K. Tashiro, *Polym. J.*, in press.
7. H. S. Fochler, J. R. Mooney, L. E. Ball, R. D. Boyer, and J. G. Grasselli, *Spectrochim. Acta*, **41A**, 271 (1985).
8. G. T. Sivy and M. M. Coleman, *Carbon*, **19**, 127 (1981).
9. I. Shimada, T. Takahagi, M. Fukuhara, K. Morita, and A. Ishitani, *J. Polym. Sci., Polym. Chem. Ed.*, **24**, 1989 (1986).
10. M. M. Coleman and R. J. Petcavich, *J. Polym. Sci., Polym. Phys. Ed.*, **16**, 821 (1978).
11. G. T. Sivy and M. M. Colemann, *Carbon*, **19**, 127 (1981).